

A nonlinear saturation model of synchronous machines with account cross saturation



Abdelaziz Salah Saidi *

Department of Electrical Engineering, King Khalid University, Abha, Saudi Arabia

ARTICLE INFO

Article history:

Received 20 January 2019

Received in revised form

25 June 2019

Accepted 27 June 2019

Keywords:

Modelling

State-space vectors

Nonlinear model

Synchronous machine

ABSTRACT

This paper developed an enhanced saturation model for synchronous machines based on simulation and experimental evaluation. The effect of taking account of cross-saturation is demonstrated. Local saturation factors are defined so as to adjust the flux-density distribution. The method of saturation modelling of dumper synchronous machine with and without cross-saturation is identified. Examples of numerical simulation are given to verify the model and its applications. Through experiments, it is shown that, by using the relationship between magnetizing current and flux as modelled in this paper, the nonlinear behavior of the synchronous machine is quite accurately estimated. Furthermore, the new model is compared with a classical model that neglects mutual saturation effects between a quadrature and direct axis windings.

© 2019 The Authors. Published by IASE. This is an open access article under the CC BY-NC-ND license (<http://creativecommons.org/licenses/by-nc-nd/4.0/>).

1. Introduction

The effects of saturation of the main flux path on the performance of electrical machines have been discussed in very many papers in the literature (Marwa et al., 2014; Khlifi et al., 2016) but there are no generalized analytical treatments of these effects. As with the theory of electrical machines before the advent of Kron's generalized theory authors tend to consider the effects of saturation in a specific machine type, and crucially the effects of intersaturation, sometimes called cross-saturation do not appear to have been included in any general analysis (Al Ahmadi et al., 2019; Singh et al., 2010).

With or without magnetic saturation, during transient operations, synchronous machines are modeled using mostly either winding currents or linkage fluxes, except for vector control purposes. In this case, two other models are generally solicited where the stator currents are mixed with the stator or rotor fluxes to achieve respectively the so-called stator or rotor flux-oriented control (Nandi, 2004; Khlifi, 2018; Singh et al., 2010). It has to be noted that, the choice of these latter kinds of models is rather dictated by the requirements of the vector control methods than the will of changing

deliberately the state variables. Obviously, when considering the different currents and fluxes as state space variables, the number of synchronous machines models is higher than known. Synthesis of possible models is rarely treated in the literature, except in Marwa et al. (2014), Khlifi et al. (2016), Levy (1986), and recently in Slimene et al. (2015a, 2015b). In all cases, the subject is treated separately for synchronous machines. In this context, it has been noticed that there are large discrepancies between the development of models with and without cross saturation of a smooth air-gap synchronous machines.

The present work is an attempt toward a comparative study of modeling cylindrical rotor synchronous machines whatever the state space variables with and without cross saturation. For that purpose, the various method of modeling saturation in the steady-state, two-axis (direct and quadrature-axis) frame models of synchronous machine are presented and compared. The magnetic coupling between the direct and quadrature-axis (magnetizing phenomenon) and its role in the analysis of the steady state performance of saturated synchronous machines are discussed (Marwa et al., 2014; Khlifi and Alshammari, 2014). A comparison between a new model, in which the effect of the cross-magnetizing phenomenon is included, and models with cross-saturation, is presented. Simulation verification of all the models for the two methods and of the inclusion of the cross-magnetizing phenomenon in the two-axis frame

* Corresponding Author.

Email Address: asaidi@kku.edu.sa<https://doi.org/10.21833/ijaas.2019.09.003>

Corresponding author's ORCID profile:

<https://orcid.org/0000-0003-1725-2418>

2313-626X/© 2019 The Authors. Published by IASE.

This is an open access article under the CC BY-NC-ND license

<http://creativecommons.org/licenses/by-nc-nd/4.0/>

models is also reported (Marwa et al., 2013; Slimene et al., 2015a, 2015b).

The paper is organized as follows. After writing the fundamental space vector equations of a round rotor synchronous machine with the usual assumptions, the extension of the procedure to introduce the magnetic saturation with and without cross saturation is contained in Section III. Section IV discusses the simulation and experimental validation of the proposed approaches as well as the equivalence between the existing models and comparisons between the two methods exposed for synchronous machine, while Section V summarizes conclusions.

2. Synchronous machine model

With the usual assumptions (Abdelaziz et al., 2011; Salah Saidi and Helmy, 2018) transient operations of damper synchronous machines with constant air gap are generally analyzed in a synchronous reference frame by the following electric equations.

$$\bar{v}_s = R_s \bar{i}_s + \frac{d\bar{\lambda}_s}{dt} + j\omega \bar{\lambda}_s \quad (1)$$

$$\bar{v}_r = R_r \bar{i}_r + \frac{d\bar{\lambda}_r}{dt} \quad (2)$$

$$\bar{v}_f = R_f \bar{i}_f + \frac{d\bar{\lambda}_f}{dt} \quad (3)$$

where,

$$\bar{\lambda}_s = l_s \bar{i}_s + \bar{\lambda}_m \quad (4)$$

$$\bar{\lambda}_r = l_r \bar{i}_r + \bar{\lambda}_m \quad (5)$$

$$\bar{\lambda}_f = l_f \bar{i}_f + \bar{\lambda}_m \quad (6)$$

and

$$\bar{\lambda}_m = L_m \bar{i}_m \quad (7)$$

$$\bar{i}_m = \bar{i}_s + \bar{i}_r + \bar{i}_f \quad (8)$$

All rotor quantities are referred to the stator. Voltages, currents and fluxes are space vectors and expressed with complex quantities. The real and imaginary parts of each space vector are known as d and q components. Because of the absence of a winding dc excitation on the quadrature axis, v_f , i_f and λ_f are real elements. If the shaft speed is not uniform, the electric Eqs. 1 to 3 must be completed by a mechanical equation. Due to the absence of the q-axis excitation winding, the number of equations in the d and q axis is not the same. Thus, it is more convenient to separate the space vector equations in d-q ones.

2.1. The d-axis equations

The direct d-axis equations of the synchronous machines are as follows:

$$v_{ds} = R_s i_{ds} + \frac{d\lambda_{ds}}{dt} - \omega \lambda_{ds} \quad (9)$$

$$0 = R_r i_{dr} + \frac{d\lambda_{dr}}{dt} \quad (10)$$

$$v_f = R_f i_f + \frac{d\lambda_f}{dt} \quad (11)$$

with

$$\lambda_{ds} = l_s i_{ds} + \lambda_{dm} \quad (12)$$

$$\lambda_{dr} = l_r i_{dr} + \lambda_{dm} \quad (13)$$

$$\lambda_f = l_f i_f + \lambda_{dm} \quad (14)$$

and

$$\lambda_{dm} = L_m i_{dm} \quad (15)$$

$$i_{dm} = i_{ds} + i_{dr} + i_f \quad (16)$$

2.2. Equations of q-axis

The direct q-axis equations of the synchronous machines are as follows:

$$v_{qs} = R_s i_{qs} + \frac{d\lambda_{qs}}{dt} + \omega \lambda_{qs} \quad (17)$$

$$0 = R_r i_{qr} + \frac{d\lambda_{qr}}{dt} \quad (18)$$

where,

$$\lambda_{qs} = l_s i_{qs} + \lambda_{qm} \quad (19)$$

$$\lambda_{qr} = l_r i_{qr} + \lambda_{qm} \quad (20)$$

$$\lambda_{qm} = L_m i_{qm} \quad (21)$$

$$i_m = i_{qs} + i_{qr} \quad (22)$$

3. Non linearity magnetic

3.1. The approach to main flux saturation modeling

The proposed common approach to introduce magnetic saturation in any d-q existing model, for the synchronous machines, relies only on the knowledge of the winding currents saturated model. For that reason, it will be first shown how to obtain it.

The leakage inductances in (4)-(6) are assumed to be constant, only the main flux $\bar{\lambda}_m$ is subject to saturation. Deriving stator and rotor linkage fluxes, in (4)-(6), leads to the time derivative of the magnetizing flux $\bar{\lambda}_m$.

$$\frac{d\bar{\lambda}_{s,r,f}}{dt} = l_{s,r,f} \frac{d\bar{i}_{s,r,f}}{dt} + \frac{d\bar{\lambda}_m}{dt} \quad (23)$$

Therefore, $\frac{d\bar{\lambda}_m}{dt}$ has to be described by means of the winding currents.

$$\frac{d\bar{\lambda}_m}{dt} = \frac{d(\lambda_m e^{i\alpha})}{dt} = e^{i\alpha} \left(\frac{d\lambda_m}{dt} + \lambda_m \frac{d\alpha}{dt} \right) \quad (24)$$

α is the angular position of $\bar{\lambda}_m$ with respect to the d-axis. It also characterizes the position of the magnetizing current \bar{i}_m in the air gap, since the hysteresis angle is neglected. Writing \bar{i}_m , α and $\frac{d\lambda_m}{dt}$ as:

$$i_m = \sqrt{i_{dm}^2 + i_{qm}^2} \quad (25)$$

$$\alpha = \tan^{-1} \frac{i_{qm}}{i_{dm}} \quad (26)$$

$$\frac{d\lambda_m}{dt} = \frac{d\lambda_m}{di_m} \frac{di_m}{dt} = L_{mdy} \frac{di_m}{dt} \quad (27)$$

we get,

$$\frac{d\lambda_{dm}}{dt} = L_{d1} \frac{di_{dm}}{dt} + L_{dq1} \frac{di_{qm}}{dt} \quad (28)$$

$$\frac{d\lambda_{qm}}{dt} = L_{dq1} \frac{di_{dm}}{dt} + L_{q1} \frac{di_{qm}}{dt} \quad (29)$$

$L_{mdy} = \frac{d\lambda_m}{di_m}$ is called dynamic inductance by analogy

with $L_m = \frac{\lambda_m}{i_m}$ said static inductance. Both coefficients are given by the conventional nonlinear magnetization curve, determined experimentally.

$$L_{dq1} = (L_{mdy} - L_m) \cos \alpha \sin \alpha \quad (30)$$

$$L_{d1} = L_m + L_{dq1} \cos \alpha \quad (31)$$

$$L_{q1} = L_m + L_{dq1} \tan \alpha \quad (32)$$

After necessary manipulations, it is not difficult to have:

$$\frac{d\lambda_{ds}}{dt} = (l_s + L_{d1}) \frac{di_{ds}}{dt} + L_{dq1} \frac{di_{qs}}{dt} + L_{d1} \frac{di_{dr}}{dt} + L_{dq1} \frac{di_{qr}}{dt} + L_{d1} \frac{di_f}{dt} \quad (33)$$

$$\frac{d\lambda_{qs}}{dt} = (l_s + L_{q1}) \frac{di_{qs}}{dt} + L_{dq1} \frac{di_{ds}}{dt} + L_{q1} \frac{di_{qr}}{dt} + L_{dq1} \frac{di_{dr}}{dt} + L_{dq1} \frac{di_f}{dt} \quad (34)$$

$$\frac{d\lambda_{dr}}{dt} = L_{d1} \frac{di_{ds}}{dt} + L_{dq1} \frac{di_{qs}}{dt} + (l_r + L_{d1}) \frac{di_{dr}}{dt} + L_{dq1} \frac{di_{qr}}{dt} + L_{d1} \frac{di_f}{dt} \quad (35)$$

$$\frac{d\lambda_{qr}}{dt} = L_{q1} \frac{di_{qs}}{dt} + L_{dq1} \frac{di_{ds}}{dt} + (l_r + L_{q1}) \frac{di_{qr}}{dt} + L_{dq1} \frac{di_{dr}}{dt} + L_{dq1} \frac{di_f}{dt} \quad (36)$$

$$\frac{d\lambda_f}{dt} = L_{d1} \frac{di_{ds}}{dt} + L_{dq1} \frac{di_{qs}}{dt} + (l_f + L_{d1}) \frac{di_f}{dt} + L_{d1} \frac{di_{dr}}{dt} + L_{dq1} \frac{di_{qr}}{dt} \quad (37)$$

The main differential system can be represented by,

$$[V] = [A][\dot{X}] + [B][X] \quad (38)$$

with,

$$[V] = [v_{ds} \ v_{qs} \ 00 \ v_f]^t \quad (39)$$

$$[X] = [i_{ds} \ i_{qs} \ i_{dr} \ i_{qr} \ i_f]^t \quad (40)$$

$$[A] = \begin{bmatrix} l_s + L_{d1} & L_{dq1} & L_{d1} & L_{dq1} & L_{d1} \\ L_{dq1} & l_s + L_{q1} & L_{dq1} & L_{q1} & L_{dq1} \\ L_{d1} & L_{dq1} & l_r + L_{d1} & L_{dq1} & L_{d1} \\ L_{dq1} & L_{q1} & L_{dq1} & l_r + L_{q1} & L_{dq1} \\ L_{d1} & L_{dq1} & L_{d1} & L_{dq1} & l_f + L_{d1} \end{bmatrix} \quad (41)$$

$$[B] = \begin{bmatrix} R_s - \omega L_s & 0 & -\omega L_m & 0 \\ \omega L_s & R_s & \omega L_m & 0 & \omega L_m \\ 0 & 0 & R_r & 0 & 0 \\ 0 & 0 & 0 & R_r & 0 \\ 0 & 0 & 0 & 0 & R_f \end{bmatrix} \quad (42)$$

It is clear that the winding currents model, which is the most known and used, is the heaviest one to compute. All 25 elements of its matrix [A] are present and saturation dependent. Also, it contains all kinds of magnetic couplings along the d-axis the q-axis L_{q1} and the d-q axis L_{dq1} . On the contrary, the winding currents model, not therefore advised, is exploited here to derive any other saturation model whatever the state-space variables.

The proposed approach consists of three stages. First, a combination of state-space vectors is chosen among the sixty-three remaining possibilities. Second, the d-q components of linkage fluxes and winding currents are described in terms of these selected variables using (12)–(15) and (19)–(21). Third, by ordinary manipulations of (33)–(37) time derivatives of the d-q components of the linkage fluxes are written as functions of the chosen variables.

3.2. Saturated model without cross-magnetizing

If magnetic saturation is accounted for, the relation binding the magnetizing current and the magnetizing flux is nonlinear, as the Fig. 1 indicates. To avoid cross-saturation complexities, in the main equations the magnetic saturation is introduced independently along the d and q axes. In addition, since the air-gap is uniform the no load magnetization curve is valid for both axes. From this latter, one can define the static and dynamic mutual inductances as in Fig. 1.

$$L_{dm} = \frac{\lambda_{dm}}{i_{dm}} \text{ and } L_{qm} = \frac{\lambda_{qm}}{i_{qm}} \quad (43)$$

$$L_{dmay} = \frac{d\lambda_{dm}}{di_{dm}} \text{ and } L_{qmay} = \frac{d\lambda_{qm}}{di_{qm}} \quad (44)$$

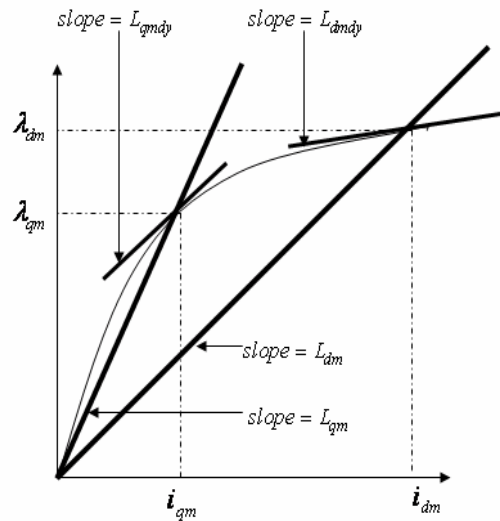


Fig. 1: Definition of static and dynamic mutual inductances for both d and q axes

For let us reasons comparative with the models with cross-saturation the choice of this model ($\bar{l}_s, \bar{l}_r, i_f$), must be identical which proceeding. So the derivation of the ($\bar{l}_s, \bar{l}_r, i_f$), model requires the description of fluxes $\bar{\lambda}_s, \bar{\lambda}_r$ and λ_f as well as their derivatives in terms of the chosen state variables.

Deriving stator and rotor linkage fluxes, we will have:

$$\begin{aligned} \frac{d\lambda_{ds}}{dt} &= l_s \frac{di_{ds}}{dt} + L_{dmay} \frac{di_{dm}}{dt} \\ \frac{d\lambda_{qs}}{dt} &= l_s \frac{di_{qs}}{dt} + L_{qmay} \frac{di_{qm}}{dt} \\ \frac{d\lambda_{dr}}{dt} &= -l_r \frac{di_{ds}}{dt} + (l_r + L_{dmay}) \frac{di_{dm}}{dt} \end{aligned} \quad (45)$$

$$\frac{d\lambda_{qr}}{dt} = -l_r \frac{di_{qs}}{dt} + (l_r + L_{qmdy}) \frac{di_{qm}}{dt} \tag{46}$$

$$\frac{d\lambda_f}{dt} = l_f \frac{di_f}{dt} + L_{dmdy} \frac{di_{dm}}{dt} \tag{47}$$

Finally the voltage equations of the $(\bar{i}_s, \bar{i}_r, i_f)$, model are:

$$[V] = [v_{ds} \quad v_{qs} \quad 00 \quad v_f]^t \tag{48}$$

$$[X] = [i_{ds} \quad i_{qs} \quad i_{dr} i_{qr} \quad i_f]^t \tag{49}$$

$$[A] = \begin{bmatrix} l_s + L_{dmdy} & 0 & L_{dmdy} & 0 & L_{dmdy} \\ 0 & l_s + L_{qmdy} & 0 & L_{qmdy} & 0 \\ L_{dmdy} & 0 & l_r + L_{dmdy} & 0 & L_{dmdy} \\ 0 & L_{qmdy} & 0 & l_r + L_{qmdy} & 0 \\ L_{dmdy} & 0 & L_{dmdy} & 0 & l_f + L_{dmdy} \end{bmatrix} \tag{50}$$

$$[B] = \begin{bmatrix} R_s & -\omega L_{ds} & 0 & -\omega L_{qm} & 0 \\ \omega L_{qs} & R_s & \omega L_{dm} & 0 & \omega L_{dm} \\ 0 & 0 & R_r & 0 & 0 \\ 0 & 0 & 0 & R_r & 0 \\ 0 & 0 & 0 & 0 & R_f \end{bmatrix} \tag{51}$$

4. Application and discussion

Though, the theory of main flux saturation is well recognized, a short application on synchronous machine is added to verify the validity of proposed method and the equivalence between models. Also, the objective of this application is to initially show comparison between models with cross magnetizing and without cross saturation moreover the equivalence between the sixty for models and then the influence of magnetic saturation on the machine operating.

For that purpose, a classical application is selected. Concerns the Build-up of the stator phase voltages for the same alternator loaded at nominal rate and which parameters are given at the end of the section.

The typical example of transients following the excitation of an isolated alternator is performed here. The aim of such application is to verify the equivalence between models and the influence of magnetic saturation. Generally, build-up of phase voltages is established at no load, but in this case all stator currents are null and the set of main equations to be solved is reduced to (2) and (3). In order to make a complete verification of the developed models, a load is added and the stator equations are implied. The alternator, which parameters are given at the end of the section, is supposed driven at rated speed. Fig. 2 illustrates the build-up process of terminal voltage of phase (a) for almost a half-loaded machine. Fig. 2 shows the excitation current of damped alternator with and without cross-saturation.

5. Conclusion

This paper has presented a comparison between two methods to develop the various models with and without cross-saturation in the synchronous machines. The saturated analytical current

model $(\bar{i}_s, \bar{i}_r, i_f)$. with and without cross magnetizing are combined for the simulation and the experimental results of synchronous machines, where numerical integration can be used to solve the nonlinear state equations.

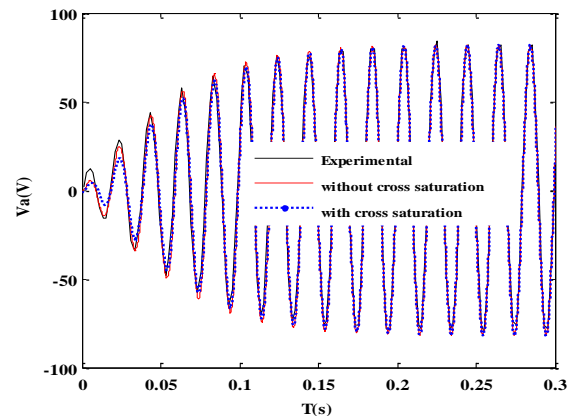


Fig. 2: Build-up of terminal voltage of an isolated and half loaded alternator

Compliance with ethical standards

Conflict of interest

The authors declare that they have no conflict of interest.

References

- Abdelaziz S, Khadija BK, Chokri B, and Mohamed E (2011). Voltage regulation and dynamic performance of the Tunisian power system with wind power penetration. Trends in Applied Science Research, 6: 813-831. <https://doi.org/10.3923/tasr.2011.813.831>
- Al Ahmadi S, Khlifi MA, and Draou A (2019). Voltage and frequency regulation for autonomous induction generators in small wind power plant. International Journal of Advanced and Applied Sciences, 6(1): 95-98. <https://doi.org/10.21833/ijaas.2019.01.013>
- Khlifi MA (2018). Behavior of a dual stator induction machine fed by neutral point clamped multilevel inverter. Journal of Energy, 2018: Article ID 6968023. <https://doi.org/10.1155/2018/6968023>
- Khlifi MA and Alshammari BM (2014). Steady state analysis of an isolated self-excited dual three-phase induction generator for renewable energy. International Journal of Modern Nonlinear Theory and Application, 3(05): 191-198. <https://doi.org/10.4236/ijmnta.2014.35021>
- Khlifi MA, Slimene MB, Fredj MB, and Rhaoulia H (2016). Performance evaluation of self-excited DFIG as a stand-alone distributed energy resources. Electrical Engineering, 98(2): 159-167. <https://doi.org/10.1007/s00202-015-0349-y>
- Levy D (1986). Analysis of a double-stator induction machine used for a variable-speed/constant-frequency small-scale hydro/wind electric power generator. Electric Power Systems Research, 11(3): 205-223. [https://doi.org/10.1016/0378-7796\(86\)90035-0](https://doi.org/10.1016/0378-7796(86)90035-0)
- Marwa BS, Mohamed AK, Mouldi BF, and Habib R (2014). Effect of the stator mutual leakage reactance of dual stator induction generator. International Journal of Electrical Energy, 2(3): 1810-1818. <https://doi.org/10.12720/ijoe.2.3.189-193>

- Marwa BS, Mohamed Arbi K, Mouldi B, and Habib R (2013). The process of self-excitation in dual three-phase induction generator. *International Review of Electrical Engineering*, 8: 1738-1744.
- Nandi S (2004). A detailed model of induction machines with saturation extendable for fault analysis. *IEEE Transactions on Industry Applications*, 40(5): 1302-1309.
<https://doi.org/10.1109/TIA.2004.834101>
- Salah Saidi A and Helmy W (2018). Artificial neural network-aided technique for low voltage ride-through wind turbines for controlling the dynamic behavior under different load conditions. *Wind Engineering*.
<https://doi.org/10.1177/0309524X18791387>
- Singh GK, Kumar AS, and Saini RP (2010). A self-excited six-phase induction generator for stand-alone renewable energy generation: Experimental analysis. *European Transactions on Electrical Power*, 20(7): 884-900.
<https://doi.org/10.1002/etep.372>
- Slimene MB, Khlifi A, Ben Fredj M, and Rehaouia H (2015a). Analysis of saturated self-excited dual stator induction generator for wind energy generation. *Journal of Circuits, Systems and Computers*, 24(9): 196-203.
<https://doi.org/10.1142/S0218126615501297>
- Slimene MB, Khlifi MA, Fredj MB, and Rehaouia H (2015b). Modeling of a dual stator induction generator with and without cross magnetic saturation. *Journal of Magnetism*, 20(3): 284-289.
<https://doi.org/10.4283/JMAG.2015.20.3.284>